

Effectiveness of Conformal Coat to Prevent Corrosion of Nickel-palladium-gold-finished Terminals

Michael Osterman

Center for Advanced Life Cycle Engineering

University of Maryland,

College Park, MD 20742

Nickel-palladium-gold-finished terminals are susceptible to creep corrosion. Excessive creep corrosion can result in device failure due to insulation resistance loss between adjacent terminals. The mixed flowing gas test has been demonstrated to produce creep corrosion on parts with nickel-palladium-gold finished terminals. Conformal coats are often used to protect printed wiring assemblies from failure due to moisture and corrosion. However, coating may not be sufficient to protect lead terminations from failure. In this study, acrylic, silicone, urethane, parylene, and atomic layer deposit (ALD) coatings were examined for their effectiveness at preventing corrosion of nickel-palladium-gold-finished terminals. The coverage of each coating was examined, and assemblies were subjected to eight hours of mixed flowing gas as well as temperature cycling. Non-uniform coating thickness was observed in the areas of the terminals. On some areas, little to no coating material was found for the acrylic, silicone, and urethane coatings. Parylene, which had the most uniform coating, was found to provide the best resistance to corrosion, while corrosion products were observed on the terminals of inspected parts protected by the other coatings.

Key words: Mixed Flowing Gas, Creep corrosion, Conformal coat **Introduction**

Conformal coatings have been widely used to mitigate failures caused by condensation and moisture spray on printed circuit boards (PCBs). The most commonly used standards for conformal coating are IPC-A-610 and IPC-CC-830. These standards give indications of good and bad coverage and outline the various failure mechanisms for coatings, such as dewetting and orange peel. However, there are no guidelines for coating coverage and how it relates to corrosion protection. The way that most suppliers control the thickness of conformal coating is by coating blank boards first in order to set their machine speeds based on a wet film gauge. Thickness measurements for the assembled PCBs are made on test coupons processed at the same time and under the same conditions. The average thickness of the coating is determined based on measurements of the flat surface at different points on the PCB. Thus, current guidelines for thickness and coverage of conformal coating may not be sufficient for assessing mitigation against corrosion-induced failures.

In examining the literature, a limited number of studies on conformal coating and its ability to mitigate corrosion have been published. Zhang et al. [1] investigated the use of urethane and parylene as conformal coatings on plastic ball grid array (BGA) packages subjected to unbiased high humidity high temperature tests. The results from these tests indicated that the parylene coating slowed down the ingress of moisture into the package, thereby delaying moisture-induced failure. The urethane coating, however, showed no advantage as a moisture barrier for high humidity conditions. Studies conducted by Zhan et al. [2] indicate that conformal coatings were found to reduce the risk of electrochemical migration, since PCBs with conformal coatings are less susceptible to surface insulation resistance degradation than uncoated PCBs. Studies conducted by Dalton et al. [3] indicated that the application of a conformal coating on surface mount resistors has a significant influence on their life when exposed to a corrosive environment such as the flowers of sulfur test. A parylene coating was also seen to improve the corrosion protection on anisotropically conductive adhesive joined flip chips subjected to salt spray tests [4]. Slaman et al. [5] employed a multi-electrode array sensor technique to monitor and assess the corrosion prevention capability of two coating materials, namely acrylic and epoxy. They found that both materials inhibited corrosion. Finally, Hindin et al. assessed seven types of conformal coating for their ability to protect silver from tarnishing and forming silver-sulfide by the flowers of sulfur test [6]. They found epoxy-type coatings provided the best protection and effectively prevented sulfur from interacting with any underlying silver alloys. Only a double coat of the urethane

acrylate provided performance similar to epoxy. None of the other coatings were able to provide sufficient protection to sulfidation if they were to be used in a high-sulfur environment during their service life.

This study examines the effectiveness of various conformal coatings in mitigating the corrosion of metallization in electronic equipment. Specifically, the corrosion of nickel-palladium-gold-finished terminals of assembled Quad Flat Packages (QFPs) is examined. Creep corrosion of nickel-palladium gold finished terminals has been reported as a concern for electronics placed in corrosive environments [7]. In order to evaluate the conformal coatings, the assemblies were subjected to environmental loading sequences in the temperature cycling test, the temperature-humidity test, and the mixed flowing gas test. After completing three exposures, the parts were examined under both optical and scanning electronic microscopes. In addition, the corrosion of lead terminals is evaluated via quantitative image analysis using SEM.

Experiments

To assess the corrosion mitigation provided by a variety of conformal coating materials, fourteen printed wiring boards with slots for sectioning attached parts were prepared. Each board had mount pads for a variety of perimeter leaded parts including quad-flat packages (QFPs), plastic leaded chip carriers (PLCCs), Small Outline Integrated Circuits (SOICs), and thin small outline packages (TSOPs). Three locations on each board included 100 terminal thin quad-flat packages (TQFPs). The nickel-palladium-gold-finished 100 terminal TQFPs were assembled with Sn-Pb solder paste. Six conformal coatings materials were examined.

Four commonly used conformal coating materials and one relatively new coating material were examined. The materials are listed in Table 1. Acrylic type 1 (AR1) and type 2(AR2), silicone (SR), and polyurethane (UR) were applied by the spray method, while parylene C(XY) and ALD-Cap O5TA200(ALD) were applied using the vacuum deposition process. ALD coating is the atomic layer deposition of an Al2O3 oxide layer with a targeted thickness of 200nm. It is known that the ALD coating is extremely smooth, pinhole-free and conforms to the underlying substrate surface [5]. Two assemblies were coated with one of the selected coatings while the two remaining assemblies were left uncoated. Each test assembly was designed so that the parts could be segmented from the assembly after the coating process. To quantify the coating, ceramic quad flat packages (CQFP) which were part of each assembly and subjected to the same assembly and coating process were destructively examined.

Table 1 Conformal coatings

| Coating Type | Coating Method |
|----------------------|-------------------|
| Acrylic 1(AR1) | Machine spray |
| Acrylic 2(AR2) | Hand spray |
| Silicone(SR) | Machine spray |
| Polyurethane(UR) | Machine spray |
| Parylene C(XY) | Vacuum deposition |
| ALD-Cap O5TA200(ALD) | Vacuum deposition |

In order to simulate a usage environment where temperature cycling and elevated temperature and humidity are present, the samples were subjected to environmental loading sequences. Further, to examine the impact of a corrosive environment, one set of samples saw corrosive exposure and the other set did not. Table 2 provides a description of the sequential loading applied to the test specimens. The specimens in both groups were subject to three kinds of temperature cycling (TC) conditions (as shown in Table 3) for 100 cycles with a 30-min dwell time. After being subjected to three series of temperature cycling conditions, the specimens in Group 1 were stored at temperature-humidity (TH) conditions with 50°C/50%RH for 200 hrs. The Group 2 specimens were exposed under the mixed flow gases (MFG) conditions with four kinds of corrosive gases (H2S, Cl2, NO2, and SO2) for 48 hrs before storing the temperature humidity conditions for 200 hrs. The modified EIA-364-TP65A Class IV was used for the MFG test and the specific conditions shown in Table 4.

Inspection for corrosion was conducted after three load cycles were completed. Prior to environmental load exposure, the specimens were inspected. Inspection included both optical and scanning electron microscopy.

Table 2 Environmental exposure sequence

| | | | | | |
|--------|------|------|------|-----|----|
| Group1 | TC-A | TC-B | TC-C | TH | |
| Group2 | TC-A | TC-B | TC-C | MFG | TH |

Table 3 Temperature cycling conditions for whisker growth

| Cycle A | | Cycle B | | Cycle C | |
|------------|-----------|------------|-----------|------------|-----------|
| Time (min) | Temp (C°) | Time (min) | Temp (C°) | Time (min) | Temp (C°) |
| 0 | 55 | 0 | 15 | 0 | 20 |
| 30 | 20 | 30 | 60 | 30 | 95 |
| 60 | 20 | 60 | 60 | 60 | 95 |
| 90 | 55 | 90 | 15 | 90 | 20 |
| 120 | 55 | 120 | 15 | 120 | 20 |

Table 4 EIA Mixed flowing gas (MFG) modified test method IV

| Class | Temp °C | RH (%) | H ₂ S (ppb) | Cl ₂ (ppb) | NO ₂ (ppb) | SO ₂ (ppb) |
|-------|---------|--------|------------------------|-----------------------|-----------------------|-----------------------|
| IV | 50 ± 2 | 75 ± 2 | 200 ± 20 | 30 ± 5 | 200 ± 50 | 200 ± 50 |

In order to calculate the coating coverage, the surfaces of two leads on each side of each CQFP (8 total for each component) were evaluated for coating coverage at four areas. The surfaces of selected leads were captured via SEM. In the SEM image, lighter-colored areas indicate material with a higher atomic number (Z); in this case, it was the metal finish devoid of coating, or covered with thinner metal coating. Imaging software was used to calculate bright and dark pixels on the images. This analysis allows for a coverage percentage to be estimated for the coatings. For the ALD coating, coverage was assessed based on the x-ray energy dispersive spectroscopy (EDS). In this case, the presence of aluminum and oxygen indicated the presence of the coating.

In addition to the surface SEM inspection, sample leads and board segments were also sectioned, and the measurement of coating thickness was conducted. Finally, after completing three complete environmental sequence loading profiles, samples were subjected to optical and SEM inspection.

Results and Discussion

Initial inspections of assembled parts prior to the environmental loading sequences showed that all spray-applied conformal coating had non-uniform coverage of lead edges compared to those that underwent the vacuum deposition method, as shown in Figure 1. Acrylic coating type 1 (AR1) showed that the pads under the leads and the sides of the leads had poor coverage compared to other spray-applied coatings. Other spray-applied conformal coatings, AR2, UR, and SR, also did not uniformly cover the edges of the leads. For conformal coating by vacuum deposition, the Parylene C and ALD coatings had uniform coating coverage, and all the surfaces, including the lead edges and pads, were fully covered by coating. Mechanical surface damage, such as scratches, were observed on both the non-coated and conformally coated samples.

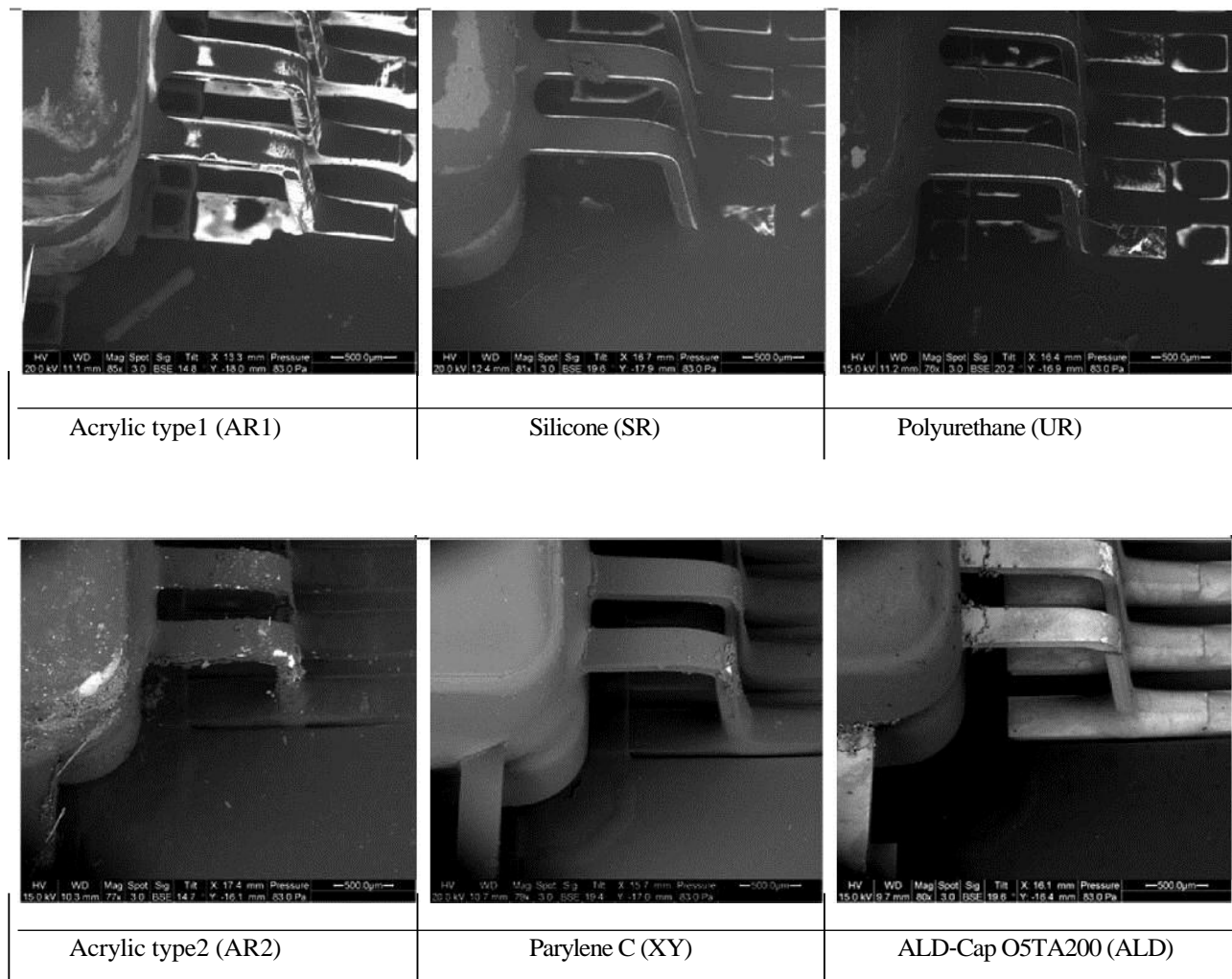


Figure 1 Initial inspection prior to environmental loading sequences.

A cross-section of a SR coated terminal, depicted in Figure 2, shows the negligible coating occurring at the edges of the terminal. Coating coverage was similar for AR1, AR2, and UR samples. The thickness of the coatings measured from cross-sections at the top surface of each terminal is provided in Table 5.

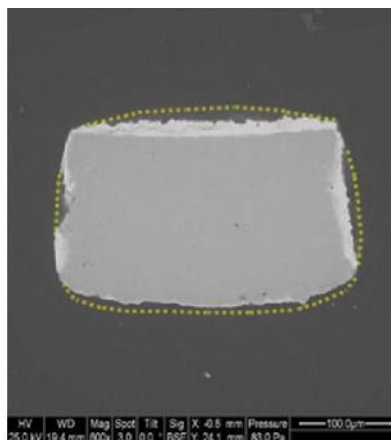


Figure 2 Cross-section of terminal with SR coating.

Table 5 Coating thicknesses

| | Application Method | Board Conformal Coating Thickness (micrometers) | Top Side Terminal Conformal Coating Thickness (micrometers) |
|------------|---------------------------|--|--|
| AR1 | Machine Spray | 20.13 (0.31) | 5.14 (1.61) |
| SR | Machine Spray | 66.45 (2.05) | 11.41 (3.39) |
| UR | Hand Spray | 27.54 (2.71) | 7.96 (1.57) |
| AR2 | Machine Spray | 33.39 (1.32) | 37.241(2.05) |
| XY | Vacuum Deposition | 17.99 (0.44) | 18.09 (2.71) |
| ALD | Vacuum Deposition | 0.1 | 0.1 |

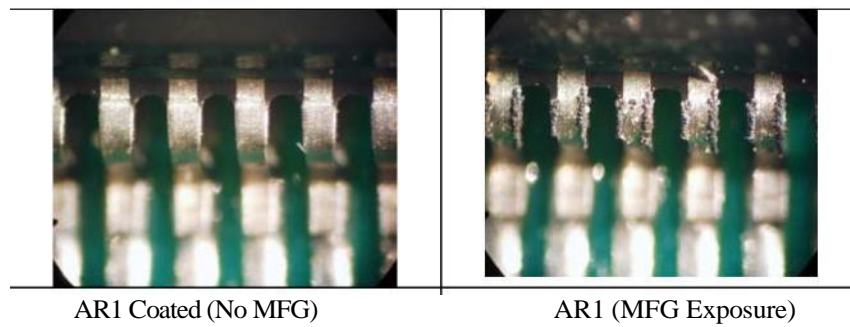


Figure 3 Optical images for AR1 coated specimens without and with MFG exposure.

After three sequential load profiles, corrosion products were observed on all specimens subjected to MFG exposure. However, corrosion products on the parylene-coated specimens were only associated with areas where the coating was damaged prior to the test due to handling. An example of optical images for AR1 coated specimens without and with manufacturing (MFG) exposure are shown in Figure 3. The worst corrosion was observed on the silicone-coated specimen. Figure 4 shows an optical image of multiple SR-coated terminals. On the SR-coated terminals, corrosion products migrated across the coated surfaces. ALD-coated terminals exhibited the next worst corrosion. Figure 5 depicts ALD coated terminals. For the urethane- and acrylic-coated specimens, the corrosion was limited to regions of poor coverage. Optical inspection of specimens after three completed cycles found no corrosion on specimens that did not undergo MFG exposure.

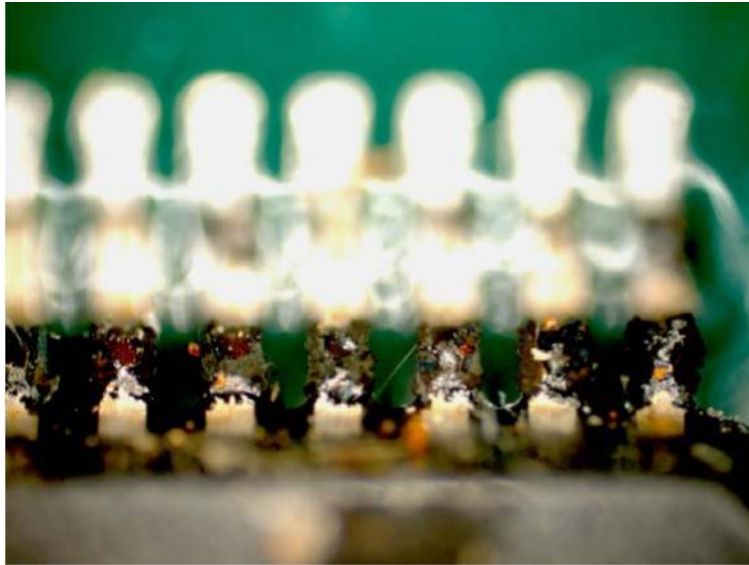


Figure 4 SR coating had copper creep corrosion over the entire surface

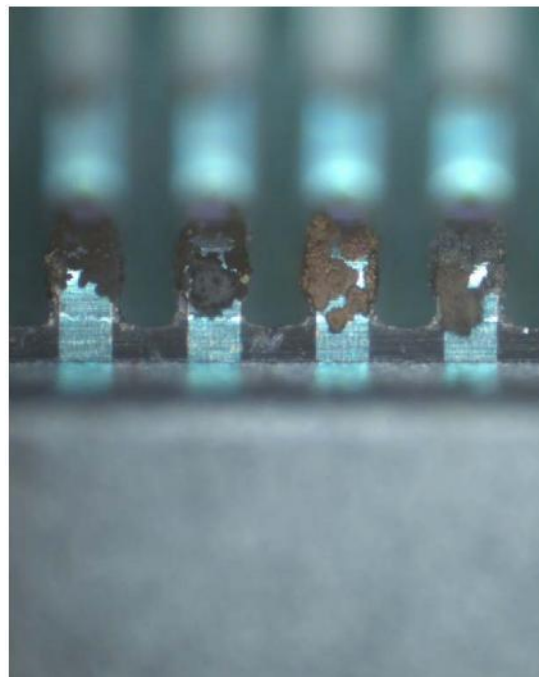


Figure 5 ALD coating showed the second most coverage of corrosion on the terminal surface.

Examination of the corrosion products under scanning electronic microscopy revealed complex corrosion structures. Figure 6 provides high magnification images of corrosion products from all sample types subjected to MFG exposure.

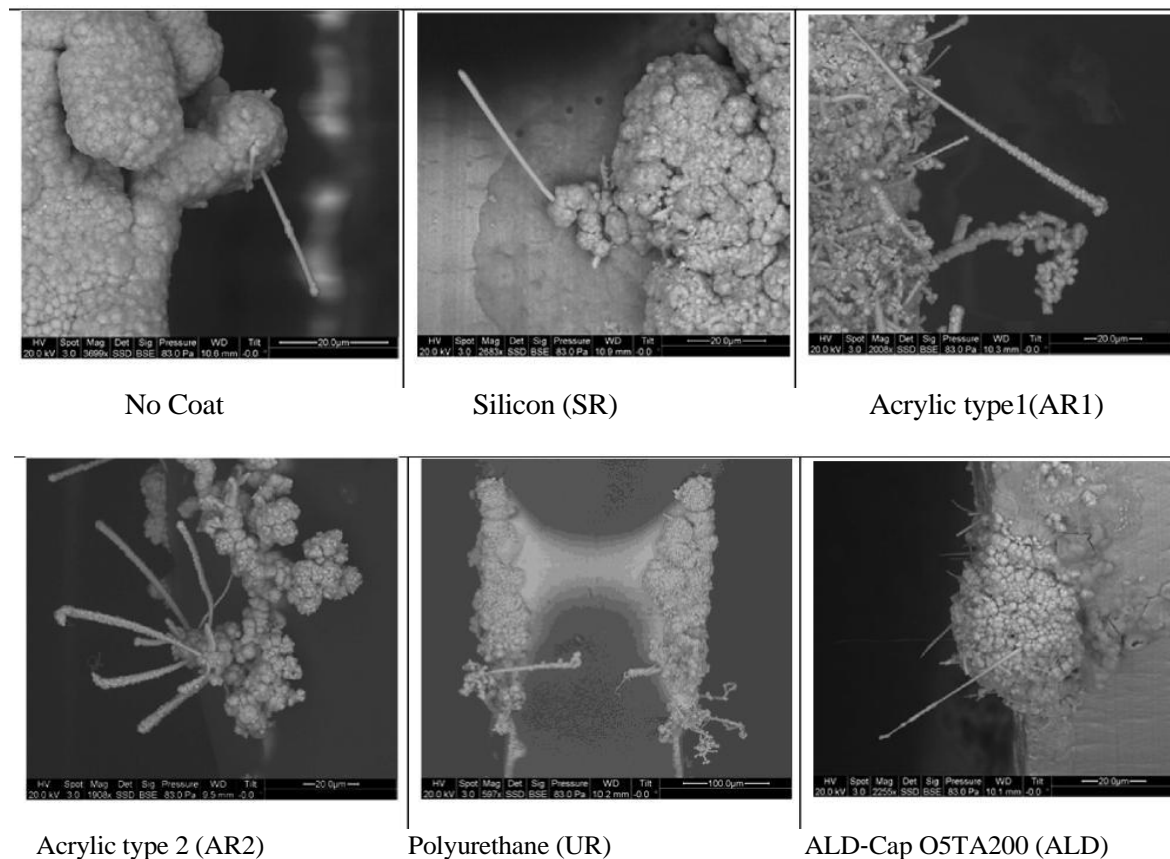


Figure 6 High magnification images of copper sulphide structures.

X-ray energy dispersive spectroscopy (EDS) of the corrosion products on all examined terminations showed they were composed of copper, sulfur, and chlorine. An elemental mapping is presented in Figure 7. The likely corrosion products were copper sulfide (Cu_2S) and copper chloride (CuCl_2).

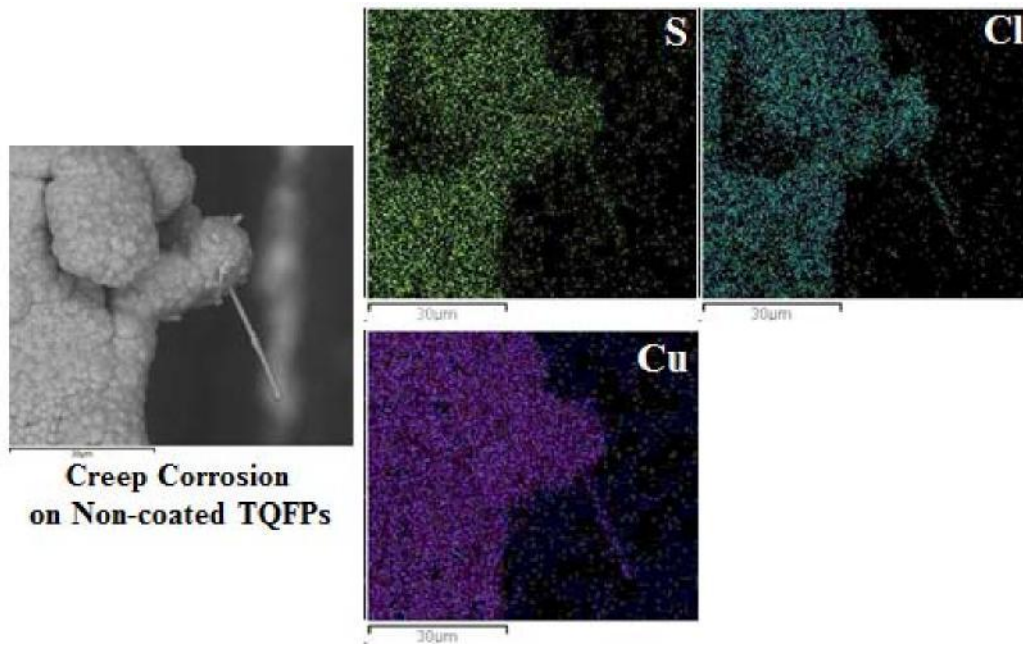


Figure 7 Energy dispersive spectrum (EDS) analysis identified copper, sulfur, and chlorine within the corrosion structure.

Conclusions

Nickel-palladium-gold-finished copper terminations are susceptible to corrosion when subjected to sulfur and chlorine gases. With the exception of parylene, the common conformal coating materials and the atomic layer deposition coating do not prevent corrosion of the terminal metallization in corrosive environments. Corrosion products were observed at regions of thinned coating thickness, in particular on the edges of the terminals. Temperature cycling may play a role in the degradation of coatings, particularly ALD, and increasing their susceptibility to corrosion. Product manufacturers with corrosive environment considerations should consider using parylene. Uniform thickness or greater thicknesses of coatings along the edges of the terminals may result in better performance for the AR, UR, and SR coatings. Manufacturers should focus on terminal coverage and not rely solely on coating thickness on a flat surface when qualifying a coating process. For this study, ALD is not recommended for mitigation of corrosion-induced failure.

References

1. K. Zhang and M. Pecht, "Effectiveness of Conformal Coatings on a PBGA Subjected to Unbiased High Humidity, High Temperature Tests", *Microelectronics International*, Vol. 17, No. 3, pp. 16-20, 2000.
2. S. Zhan, M. Azarian, and M. Pecht, "Surface Insulation Resistance of Conformally Coated Printed Circuit Boards Processed With No-Clean Flux", *IEEE Transactions on Electronics Packaging Manufacturing*, Vol. 29, No. 3, pp. 217-233, July 2006.
3. E. Dalton, M. Collins, M. Reid, J. Punch, "Conformal Coating Protection Of Surface Mount Resistors In Harsh Environments", *Proceedings of ICSR (International Conference on Soldering and Reliability)*, 2012.
4. K. Kokko, A. Parviainen, L. Frisk, "Corrosion protection of anisotropically conductive adhesive joined flip chips", *Microelectronics Reliability*, Vol. 50, pp 1152–1158, 2010.
5. A. Salman, Z. Burhanudin and N. Hamid, "Effects of Conformal Coatings on the Corrosion Rate of PCB-based Multielectrode-Array-Sensor", *2010 International Conference on Intelligent and Advanced Systems*.
6. B. Hindin, J. Fernandez, "Testing of Conformal Coatings Using the Flowers-of-Sulfur Test", *2003 Tri-Service Corrosion Conference*.
7. J. Xie and M. Pecht, *Palladium-plated Packages: Creep Corrosion and Its Impact on Reliability*, *Advanced Packaging*, pp. 39-42, February 2001.